

Bayesian Additive Regression Tree Copula Processes for Scalable Distributional Prediction

Jan Martin Wenkel¹, Michael Stanley Smith² and Nadja Klein¹

¹Scientific Computing Center, Karlsruhe Institute of Technology, Germany

²Melbourne Business School, University of Melbourne, Australia

Abstract

We show how to construct the implied copula process of response values from a Bayesian additive regression tree (BART) model with prior on the leaf node variances. This copula process, defined on the covariate space, can be paired with any marginal distribution for the dependent variable to construct a flexible distributional BART model. Bayesian inference is performed via Markov chain Monte Carlo on an augmented posterior, where we show that key sampling steps can be realized as those of Chipman et al. (2010), preserving scalability and computational efficiency even though the copula process is high dimensional. The posterior predictive distribution from the copula process model is derived in closed form as the push-forward of the posterior predictive distribution of the underlying BART model with an optimal transport map. Under suitable conditions, we establish posterior consistency for the regression function and posterior means and prove convergence in distribution of the predictive process and conditional expectation. Simulation studies demonstrate improved accuracy of distributional predictions compared to the original BART model and leading benchmarks. Applications to five real datasets with 506 to 515,345 observations and 8 to 90 covariates further highlight the efficacy and scalability of our proposed BART copula process model.

Keywords: BART, Copula Process, Distributional Regression, Implicit Copula, Transport Map

Corresponding author: Prof. Dr. Nadja Klein, Scientific Computing Center, Karlsruhe Institute of Technology, Zirkel 2, 76131 Karlsruhe, Germany, nadja.klein@kit.edu.

Acknowledgments: Nadja Klein acknowledges support through the Emmy Noether grant KL 3037/1-1 of the German research foundation (DFG). Michael Smith’s research has been partially supported by the Australian Research Council (ARC) Discovery Project grant DP250101069. This work has been supported by the German Federal Ministry of Research, Technology and Space (BMFTR) within the project “CausalNet”, grant no. 01IS24082

1 Introduction

Bayesian Additive Regression Trees (BART), introduced by Chipman et al. (2010), is a popular scalable nonparametric approach to regression and classification; see Hill et al. (2020) for a review. BART models the regression function as a sum of regression trees, each constrained by a regularization prior to act as a weak learner (Schapire; 1990). The ensemble of the weak learner trees can capture complex nonlinear relationships and interactions, and provides strong predictive performance in high-dimensional and sparse settings; see Chipman et al. (2010); Kapelner and Bleich (2016); He et al. (2019) for extensive empirical evidence.

A major reason for the success of BART is that it is a well-defined stochastic model that allows for Bayesian uncertainty quantification, along with fast evaluation of posterior inference and prediction. It is also easy to extend, and there is a large literature doing so over the past decade. Methodological developments include adaptations to enforce monotonicity constraints (Chipman et al.; 2022), assess sensitivity to violations in modeling assumptions (Pratola et al.; 2024), allow for missing data (Linero and Daniels; 2015), smoother functions (Linero and Yang; 2018) and variable selection and shrinkage (Wang et al.; 2022; Linero and Du; 2023), including in high-dimensions (Linero; 2018). Extensions to models for causal inference (Hill et al.; 2013; Hahn et al.; 2020), survival analysis (Basak et al.; 2022; Linero et al.; 2022), and spatial modeling (Scarpone et al.; 2020; Ghosh et al.; 2024), broaden the applicability of BART. In this paper, we consider its extension to distributional regression and prediction using a novel copula process model.

Distributional regression is where the entire distribution of the response variable is modeled as a function of the covariates. It is suitable whenever the response distribution may be heteroscedastic, skewed, heavy-tailed, and/or multi-modal; features which occur in many contemporary applications, see Klein (2024) for an overview. In this paper, we propose a framework for distributional prediction based on a Gaussian copula process on the covariate space. The copula process is the implicit copula of the response values from a BART model with Gaussian disturbances, and is conditional on the covariates. We call these “pseudo-response” values because they are not observed directly. For the copula process to be effective, we assume a prior on the leaf node variances and derive the distribution of

pseudo-response values with the leaf nodes integrated out. This approach extends the implicit copulas for regularized linear regression models suggested by Klein and Smith (2019) and Smith and Klein (2021). The proposed copula process can then be combined with any marginal distribution for the observed response variable to define a copula process model that is a flexible distributional regression approach that we label “CP-BART”. Predictions are given by the posterior predictive distribution, which we show is the push-forward of the posterior predictive distribution of the pseudo-response under a transport map that is optimal with respect to quadratic cost. Computation of the predictive distribution and posterior inference use a Markov chain Monte Carlo (MCMC) algorithm that shares key steps with the original sampler of Chipman et al. (2010) and is equally scalable.

Under mild regularity conditions, we establish posterior consistency. Building on the results of Ročková and van der Pas (2020), who establish posterior concentration properties of the BART model under specific assumptions (most notably the α -Hölder continuity of the regression function f_0 for $0 < \alpha \leq 1$) we first show posterior concentration for the BART model of the pseudo response, where we allow for a prior on the leaf node variances. This additional layer of flexibility improves predictive accuracy of our CP-BART model. We next show posterior convergence in distribution of the conditional distribution estimates, and, under sufficiently strong tail decay of the responses, that the point estimates of the CP-BART model converge in probability to the conditional expectation of the responses. To establish these results, we require consistent estimators for f_0 and the leaf node variances. Under additional assumptions, we then prove that their posterior means are indeed consistent estimators.

The finite sample performance of CP-BART is assessed through both simulation studies and five real world datasets with between 506 and 515,345 observations on 8 to 90 covariates. Density forecasts from CP-BART are more accurate than those from the original BART model of Chipman et al. (2010) and two established benchmark methods for distributional prediction. They are smoother, sharper and/or better located, with a mean pinball (check) loss function that shows they are more accurate at all quantiles in all five real world examples. Following Li et al. (2023), we also show that CP-BART conditional quantile coverage is more accurate, indicating accurate epistemic uncertainty quantification.

Our paper is not the first to suggest extending BART to distributional regression. Linero (2025) proposed an approach that is applicable to arbitrary parametric distributions assuming the log-density and its derivatives can be provided. While this framework is very flexible, it requires the choice of a set of potential distributions and a parametric assumption that may not hold in practice. A nonparametric alternative is suggested by O’Hagan and Ročková (2025) who propose a generative regression based on the implicit quantile BART model. This model is different to ours since it targets the conditional quantile function rather than a density forecast. Inference is obtained by a data augmentation approach which can be computationally expensive with increasing sample size. In addition, the authors rely on the asymmetric Laplace distribution which they frame as a Gibbs posterior (Bissiri et al.; 2016) with uncertainty quantification over the quantile function. To avoid quantile crossing in the model by O’Hagan and Ročková (2025), the original BART prior needs to be adapted to ensure monotonicity, something that is unnecessary with our approach.

Our method is also related to other distributional regression models employing BART that do not require a parametric assumption, while modelling the entire distribution. Orlandi et al. (2021) consider a covariate-dependent mixture model for a latent variable. This work is related to the adaptive conditional density estimation model of Li et al. (2023), who model the conditional density of the response by tilting a base model and modelling the regression function via the soft decision tree of Linero and Yang (2018). While not the focus of this paper, it is conceptually also possible to extend our approach to multivariate responses. An example of such a multivariate response model with BART is that of Um et al. (2023), who consider the multivariate skew normal distribution with a multivariate BART prior.

The rest of the paper is structured as follows. Sections 2 and 3 detail the proposed model and efficient Bayesian estimation, respectively. In Section 4 we establish posterior consistency. Sections 5 and 6 evaluate our CP-BART model empirically in simulations and real world data illustrations. Section 7 concludes by highlighting the contributions of our work and directions for further work.

2 Proposed Model

In this section we first briefly specify the BART model, introducing the necessary notation for our theoretical results in Section 4, and the priors that we adopt. We then write it as a Gaussian linear model, which is used to construct the implicit copula process of its response values. Finally, we show how to construct the posterior predictive distribution from the copula process model with arbitrary marginals using a transport map. This is the basis of our proposed distributional BART model.

2.1 Bayesian Additive Regression Trees

BART was introduced by Chipman et al. (2010) and is an extension of classical sum of trees models in which the unknown regression function is modelled as a flexible ensemble of trees.

Regression Tree: A single tree with partition $\mathcal{T} = \{T_k\}_{k=1}^K$ of the unit cube $[0, 1]^p$ for n realizations x_1, \dots, x_n of a p -dimensional independent variable vector (standardized to the unit cube), has empirical measure

$$\mu(T_k) = \frac{1}{n} \sum_{i=1}^n \mathbb{1}_{T_k}(x_i),$$

where the indicator function $\mathbb{1}_A(x) = 1$ if $x \in A$ and zero otherwise. A tree partition is called valid if it satisfies

$$\mu(T_k) \geq \frac{C_0^2}{n} \quad \text{for all } k = 1, \dots, K$$

for some constant $C_0^2 \in \mathbb{N} \setminus \{0\}$. Now consider the function space containing all possible step functions from valid tree partitions defined as

$$\mathcal{F}_{\mathcal{T}} = \bigcup_{q=0}^{\infty} \bigcup_{K=1}^{\infty} \bigcup_{Q:|Q|=q} \mathcal{F}(\mathcal{V}_Q^K),$$

where \mathcal{V}_Q^K denotes the family of valid tree partitions with K cells splitting each x_i at least once. Here, $Q \subseteq \{1, \dots, p\}$ with $|Q| = q \leq p$ denotes the number of “active” covariates that determine the splits. Thus, $\mathcal{F}_{\mathcal{T}}$ is the union over all possible numbers of active predictors, tree sizes and partitions.

For a tree partition $\mathcal{T} \in \mathcal{V}_Q^K$ with leaf node values denoted as $M = (\mu_1, \dots, \mu_K)^\top \in \mathbb{R}^K$,

the associated set of tree-structured step functions is defined by

$$\mathcal{F}(\mathcal{V}_Q^K) = \left\{ f_{\mathcal{T},M} : [0, 1]^p \rightarrow \mathbb{R}; f_{\mathcal{T},M}(x) = \sum_{k=1}^K \mu_k \mathbb{1}_{T_k}(x), \text{ where } \mathcal{T} \in \mathcal{V}_Q^K, M \in \mathbb{R}^K \right\}.$$

Additive Regression Tree: An additive regression tree model extends a single tree by combining m trees into an ensemble. For tree j , let $Q^j \subseteq \{1, \dots, p\}$ be its $|Q^j| = q^j$ active covariate indices, and K^j be the number of terminal nodes. If $f_{\mathcal{T}^j, M^j} \in \mathcal{V}_{Q^j}^{K^j}$ denotes the step function associated with tree j , a regression forest can be defined as the ensemble

$$f_{\mathcal{E}, \mathcal{M}}(x) = \sum_{i=1}^m f_{\mathcal{T}^i, M^i}(x),$$

where $\mathcal{E} = \{\mathcal{T}^1, \dots, \mathcal{T}^m\}$ is the set of trees in the ensemble and $\mathcal{M} = (M^1, \dots, M^m)^\top$ is the vector of all the leaf nodes in the ensemble.

Moreover, if the covariate indices $\mathcal{Q} = \{Q^1, \dots, Q^m\}$ and tree sizes $\mathcal{K} = (K^1, \dots, K^m)^\top$, we use $\mathcal{V}_{\mathcal{Q}}^{\mathcal{K}}$ to denote the ensemble of tree partitions \mathcal{T}^j , $j = 1, \dots, m$. We can then define the function spaces $\mathcal{F}(\mathcal{V}_{\mathcal{Q}}^{\mathcal{K}})$ and $\mathcal{F}(\mathcal{E})$ as

$$\mathcal{F}(\mathcal{V}_{\mathcal{Q}}^{\mathcal{K}}) = \left\{ f_{\mathcal{E}, \mathcal{M}} : [0, 1]^p \rightarrow \mathbb{R}; f_{\mathcal{E}, \mathcal{M}}(x) = \sum_{j=1}^m f_{\mathcal{T}^j, M^j}(x); \mathcal{E} \in \mathcal{V}_{\mathcal{Q}}^{\mathcal{K}}, M^j \in \mathbb{R}^{K^j} \right\},$$

and

$$\mathcal{F}(\mathcal{E}) = \bigcup_{m=1}^{\infty} \bigcup_q \bigcup_{\mathcal{Q}: |\mathcal{Q}|=q} \bigcup_{\mathcal{K}} \mathcal{F}(\mathcal{V}_{\mathcal{Q}}^{\mathcal{K}}).$$

Prior distributions: A defining feature of BART is that the prior regularizes each tree so that it behaves as a “weak learner” (Schapire; 1990; Chipman et al.; 2010) where no single tree explains much of the variation, and only the sum produces a flexible model. This is achieved through hierarchical priors on the structure and leaf values of each tree. For the number of active predictors $q^j = |Q^j|$ in each tree j , we assume the prior

$$\pi(q^j) \propto C^{-q^j} p^{Aq^j}, \quad \text{for } q^j = 0, 1, \dots, p,$$

and some constants $A, C > 0$. Conditional on q_j , a uniform prior on Q^j is assumed, so that

$$\pi(Q^j | q^j) = \binom{p}{q^j}^{-1}.$$

Following Ročková and Saha (2019), the prior on the number of terminal nodes K^j follows a Galton–Watson branching process with node-specific splitting probability $p_{split}(k) = \alpha^{d(k)}$

where $d(k)$ denotes the depth of node k in the tree, $0 < \alpha \leq 1$. Given \mathcal{Q} and \mathcal{K} , a (conditionally) uniform prior is placed on the tree topologies \mathcal{E} :

$$\pi(\mathcal{E} \mid \mathcal{Q}, \mathcal{K}) = \frac{1}{|\mathcal{V}\mathcal{E}_{\mathcal{Q}}^{\mathcal{K}}|} \mathbb{1}_{\mathcal{V}\mathcal{E}_{\mathcal{Q}}^{\mathcal{K}}}(\mathcal{E}).$$

Finally, independent zero mean Gaussian priors on the leaf node values of each are assumed. We also do so when constructing the copula process, but where the variance is selected differently than in Chipman et al. (2010), as discussed further below.

Remark 1. The prior on K^j differs from that originally adopted by Chipman et al. (2010). Ročková and Saha (2019) show the original prior provides insufficient decay of the tail of the distribution of tree sizes to achieve the bound at (C.3) in the Supplementary Material, which is required to prove posterior consistency in Section 4. Moreover, we found both the original and adopted priors give very similar results empirically.

2.2 BART Copula Process Model

With Gaussian disturbances, we write BART as a Bayesian linear model from which its implicit copula process is then constructed. We then show that the copula process is interpretable as a transport map, which then allows for efficient Bayesian inference in Section 3. When the copula process is combined with an arbitrary marginal for a dependent variable, the resulting copula process model is shown to provide flexible distributional predictions.

BART Linear Model: Consider the following regression for a response \tilde{Z}_i (which we call the “pseudo response”) with independent additive Gaussian disturbances

$$\tilde{Z}_i = f_0(x_i) + \varepsilon_i, \quad \varepsilon_i \sim \mathcal{N}(0, \sigma^2), \quad (1)$$

for $i = 1, 2, \dots, n$. The mean function f_0 is unknown, and we model it using BART as follows. Recall that M^j is the vector of leaf node values of the ensemble member j . Then let E^j be a $(n \times K^j)$ matrix of zeroes and ones that selects the elements of M^j , such that

$$\mathbf{f}_{\mathcal{T}^j, M^j} := \left(f_{\mathcal{T}^j, M^j}(x_1), \dots, f_{\mathcal{T}^j, M^j}(x_n) \right)^\top = E^j M^j. \quad (2)$$

If $E = [E^1 \mid E^2 \mid \dots \mid E^m]$, then the ensemble evaluated at the n observations can be written as

$$(f_0(x_1), \dots, f_0(x_n))^\top = (f_{\mathcal{E}, \mathcal{M}}(x_1), \dots, f_{\mathcal{E}, \mathcal{M}}(x_n))^\top = \sum_{j=1}^m \mathbf{f}_{\mathcal{T}^j, M^j} = EM.$$

Conditional on $\{\mathcal{E}, \mathcal{M}, \sigma^2\}$, the pseudo response vector $\tilde{Z}_{1:n} = (\tilde{Z}_1, \dots, \tilde{Z}_n)^\top$ follows the linear model

$$\tilde{Z}_{1:n} | \mathcal{E}, \mathcal{M}, \sigma^2 \sim \mathcal{N}(EM, \sigma^2 I_n). \quad (3)$$

where I_n is the $n \times n$ identity matrix, and the trees \mathcal{E} summarize all the information in the covariates $x_{1:n} = \{x_1, \dots, x_n\}$. We adopt the BART prior as outlined previously. For the leaf node values we choose independent Gaussian priors of the form

$$M^j | c, \sigma^2 \sim \mathcal{N}(0, c\sigma^2 I_{K^j}), \quad j = 1, \dots, m, \quad (4)$$

where $c > 0$. The prior variance differs from that adopted by Chipman et al. (2010) in two ways. First, scaling by σ^2 simplifies its integration out of the copula process, where later it is shown to be unidentified. Second, in contrast to the standard BART model, the scale of the leaf node values are hard to determine a priori in the copula process. Therefore, we also estimate the scale parameter c , for which we adopt the inverse gamma prior $c \sim \mathcal{IG}(a, b)$, with shape and scale parameters a, b . We show later posterior consistency under this prior, how to select a, b , and that this additional layer of flexibility improves predictive accuracy from the copula model.

Gaussian Copula Process: Every multivariate continuous distribution has a unique copula that fully captures its dependence structure, widely called its “implicit copula” (Smith; 2023). We employ the implicit copula of the conditional distribution of $\tilde{Z}_{1:n}$ with the leaf node values marginalized out given by

$$\tilde{Z}_{1:n} | \mathcal{E}, c, \sigma^2 \sim \mathcal{N}(0, \sigma^2(cEE^\top + I_n)). \quad (5)$$

The implicit copula of a Gaussian distribution is the popular Gaussian copula and its parameter is the correlation matrix of the distribution; see Song (2000). Some simple computations show that the correlation matrix of (5) is $\Omega = S_{1:n}(cEE^\top + I_n)S_{1:n}$, where the scaling matrix

$S_{1:n} = sI_n$ with $s = \text{var}(\tilde{Z}_i)^{-1/2} = (1 + mc)^{-\frac{1}{2}}$.

Let $u_{1:n} \in [0, 1]^n$ and $z_{1:n} = \underline{\Phi}^{-1}(u_{1:n})$, where $\underline{\Phi}^{-1}$ denotes elementwise application of the standard normal quantile function. Then the density of the Gaussian copula process is

$$c_{\text{Ga}}(u_{1:n}; \Omega(c, \mathcal{E})) = |\Omega(c, \mathcal{E})|^{-1/2} \exp\left(-\frac{1}{2} z_{1:n}^\top (\Omega(c, \mathcal{E})^{-1} - I_n) z_{1:n}\right), \quad (6)$$

and we make three observations. First, Ω is not a function of σ^2 , which shows that the scale of \tilde{Z}_i is unidentified in the copula. Therefore, without loss of generality, we set $\sigma = 1$ in (1) throughout. Second, Ω is a function of c, \mathcal{E} , which are the only parameters of our Gaussian copula process. Therefore, we sometimes write $\Omega(c, \mathcal{E})$ for Ω , and later show how to use their Bayesian posterior for inference on their values. Third, marginalizing the leaf node values \mathcal{M} out of (5) is necessary when constructing the copula process. If it was not, then the implicit copula of $\tilde{Z}_{1:n} | \mathcal{E}, c, \sigma^2, \mathcal{M}$ at (3) is simply the independence copula, which provides uninformative predictions of future observations.

Prior Scaling: Unlike with the standard BART model, which has a fixed variance for the leaf node values, we adopt the hyperprior $c \sim \mathcal{IG}(a, b)$. Following Klein and Kneib (2016), setting $a = 1$ mimics a proper but relatively uninformative prior for $1/c$. The hyper-parameter b is set to capture available prior knowledge. Based on the observation that $\tilde{z}_i | x_{1:n} \sim N(0, 1 + mc)$, approximately 99% of pseudo-observations lie in the interval $(-3\sqrt{1 + mc}, 3\sqrt{1 + mc})$. We choose c such that $\pm k$ -times the standard deviation of the sum of all the leaf node values still lie within this interval, where we set $k = 4$. Solving this equation for c gives an optimal value

$$k\sqrt{mc} = 3\sqrt{1 + mc} \quad \Leftrightarrow \quad c = \frac{9}{(k^2 - 9)m},$$

so that $k = 4$ results in $c^* = \frac{9}{7m}$. The hyper-parameter b is chosen so that the mode of the prior distribution is c^* . The mode of a $\mathcal{IG}(1, b)$ distribution is $\frac{b}{2}$, therefore the optimal b is given by $b^* = \frac{9}{14m}$.

Copula Process Model: The copula process model combines the BART copula process above with marginals for the observed response. Consider regression data $\{(Y_i, x_i)\}_{i=1}^n$, where $Y_i \in \mathbb{R}$ is the dependent variable. We make the usual regression assumption that

$Y_i|x_{1:n} \stackrel{d}{=} Y_i|x_i$ for $1 \leq i \leq n$, and denote its distribution function as $F_{Y_i}(y_i|x_i)$ and density as $p_{Y_i}(y_i|x_i) = \frac{d}{dy_i} F_{Y_i}(y_i|x_i)$. By Sklar's theorem, the joint density of $Y_{1:n} = (Y_1, \dots, Y_n)^\top$ conditional on $x_{1:n}$ is

$$p(y_{1:n}|x_{1:n}) = c^\dagger(F_{Y_1}(y_1|x_1), \dots, F_{Y_n}(y_n|x_n); x_{1:n}) \prod_{i=1}^n p_{Y_i}(y_i|x_i), \quad (7)$$

for some n -dimensional copula with density $c^\dagger(u_{1:n}; x_{1:n})$.

In the copula modeling literature, a parametric copula is usually selected for c^\dagger . In this paper, we propose adopting the Gaussian copula process implicit in the BART model discussed above, and set $c^\dagger(u_{1:n}; x_{1:n}) = c_{\text{Ga}}(u_{1:n}; \Omega(c, \mathcal{E}))$. In the BART model the effect of the covariates is summarized by the tree ensemble \mathcal{E} , and it is here too. Following Klein and Smith (2019) and Smith and Klein (2021) we also assume the marginals are invariant to x_i , so that $F_{Y_i}(y_i|x_i) := F_Y(y_i)$. This has the advantage that F_Y can be estimated separately from the copula parameters non-parametrically. (Later, this assumption also means that it is solely the copula process that captures the impact of the covariates in the distributional predictions.) Our copula model for (7) is therefore

$$p(y_{1:n}|x_{1:n}) = p(y_{1:n}|c, \mathcal{E}) = c_{\text{Ga}}(F_Y(y_1), \dots, F_Y(y_n); \Omega(c, \mathcal{E})) \prod_{i=1}^n p_Y(y_i). \quad (8)$$

with $p_Y(y) = \frac{d}{dy} F_Y(y)$.

Copulas are also interpretable as transport maps (Kolesárová et al.; 2008). The following proposition is useful for computing efficiently both the posterior of the copula parameters, and also the predictions from the model.

Proposition 1. *Let A be a set of realization indices (e.g. $A = \{1 : n\}$, $A = \{i\}$ or $A = \{n + 1\}$). Consider the element-wise transport map R at these indices given by*

$$y_A = R(\tilde{z}_A) := \underline{F}_Y^{-1}(\underline{\Phi}(S_A \tilde{z}_A)), \quad (9)$$

where $S_A = sI_{|A|}$ is the scaling matrix defined above, and \underline{F}_Y^{-1} and $\underline{\Phi}$ denote element-wise application of the quantile function F_Y^{-1} and distribution function Φ , respectively. Then the determinant of the Jacobian of the transformation is

$$\det(J_R) := \left| \frac{dy_A}{dz_A} \right| = \prod_{i \in A} \frac{s\phi(z_i)}{p_Y(y_i)},$$

where $z_i = s\tilde{z}_i$ is the standardized value of the pseudo-response, and ϕ is the standard normal

density. Moreover, if \mathbb{P}_X denotes the probability measure of the distribution of random vector X , then

(i) R pushes $\mathbb{P}_{\tilde{Z}_A|c,\mathcal{E}}$ forward to $\mathbb{P}_{Y_A|c,\mathcal{E}}$ and is the optimal transport under quadratic loss, and

(ii) R pushes $\mathbb{P}_{\tilde{Z}_A|c,\mathcal{E},\mathcal{M}}$ forward to $\mathbb{P}_{Y_A|c,\mathcal{E},\mathcal{M}}$.

Part (i) shows that R is the canonical transformation underlying the Gaussian copula process model with density at (8). Part (ii) is important as we employ it to evaluate posterior inference and predictions efficiently using augmentation with the leaf nodes \mathcal{M} below. The proof of Proposition 1 is provided in the Supplementary Material Part A.

2.3 Prediction

Distributional, point and quantile predictions can all be obtained from the BART copula process model.

Distributional Predictions: The posterior predictive distribution of an unobserved value of the dependent variable Y_{n+1} given observed covariates x_{n+1} can be computed as follows. Let $\eta = \{c, \mathcal{E}, \mathcal{M}\}$ denote the copula parameters augmented with the leaf node values, and $A = \{n + 1\}$ be a singleton set in (9). Then it follows from Part (ii) of Proposition 1 and the regression at (1) (with $\sigma = 1$) that the posterior predictive distribution is

$$\begin{aligned} p_{n+1}(y_{n+1}|x_{n+1}) &:= \int p(y_{n+1}|x_{n+1}, \eta)p(\eta|y_{1:n})d\eta \\ &= \int p(\tilde{z}_{n+1}|x_{n+1}, \eta) \det(J_R^{-1})p(\eta|y_{1:n})d\eta \\ &= \int \phi(\tilde{z}_{n+1} - f_{\mathcal{E},\mathcal{M}}(x_{n+1})) \frac{p_Y(y_{n+1})}{s\phi(z_{n+1})} p(\eta|y_{1:n})d\eta, \end{aligned} \quad (10)$$

where

$$\tilde{z}_{n+1} = R^{-1}(y_{n+1}) = \Phi^{-1}(F_Y(y_{n+1}))/s.$$

The integral at (10) can be evaluated in the usual Bayesian fashion to obtain an estimator $\hat{p}_{n+1}(y_{n+1}|x_{n+1})$ using draws from the augmented posterior $\eta^{[k]} \sim p(\eta|y_{1:n})$, for which we suggest an efficient MCMC sampling scheme in Section 3 below. An alternative “plug in”

estimator replaces s and $f_{\mathcal{E},\mathcal{M}}(x_{n+1})$ with their Monte Carlo estimates $\bar{s} = (1 + m\bar{c})^{-1/2}$, $\bar{c} = \frac{1}{K} \sum_{k=1}^K c^{[k]}$ and $\bar{f}_{\mathcal{E},\mathcal{M}}(x_{n+1}) = \frac{1}{K} \sum_{k=1}^K f_{\mathcal{E}^{[k]},\mathcal{M}^{[k]}}(x_{n+1})$ constructed from K draws from the augmented posterior. Although this under-represents posterior uncertainty, it is faster to evaluate and we find in our empirical work that it gives very similar distributional predictions.

Mean Predictions: The posterior predictive mean

$$\mathbb{E}(Y_{n+1}|x_{n+1}) := \int \mathbb{E}(Y_{n+1}|x_{n+1}, \eta) p(\eta|y_{1:n}) d\eta. \quad (11)$$

(i.e., the mean of (10)) can be used as a point prediction of Y_{n+1} given a new covariate value x_{n+1} . The integral can be computed using the draws $\eta^{[k]}$ from the augmented posterior to obtain an estimator $\widehat{Y}_{n+1}(x_{n+1})$. However, as before we adopt the faster alternative of using the plug-in posterior mean estimators \bar{s} and $\bar{f}_{\mathcal{E},\mathcal{M}}(x_{n+1})$. Using Part (ii) of Proposition 1 with index set $A = \{n+1\}$, and observing from (1) that $\widetilde{Z}_{n+1} \sim N(f_{\mathcal{E},\mathcal{M}}(x_{n+1}), 1)$, it follows that the term in the integrand of (11) is

$$\begin{aligned} \mathbb{E}(Y_{n+1}|x_{n+1}, \eta) &= \int y_{n+1} p(y_{n+1}|x_{n+1}, \eta) dy_{n+1} \\ &= \int y_{n+1} \phi(\tilde{z}_{n+1} - f_{\mathcal{E},\mathcal{M}}(x_{n+1})) \frac{p_Y(y_{n+1})}{s\phi(z_{n+1})} dy_{n+1}. \end{aligned}$$

Changing the variable of integration to $z_{n+1} = s\tilde{z}_{n+1} = \Phi^{-1}(F_Y(y_{n+1}))$ gives

$$\mathbb{E}(Y_{n+1}|x_{n+1}, \eta) = \int F_Y^{-1}(\Phi(z_{n+1})) \phi(z_{n+1}/s - f_{\mathcal{E},\mathcal{M}}(x_{n+1})) dz_{n+1}.$$

which is evaluated using univariate numerical integration.

Quantile Predictions: The posterior predictive quantile $Q_{n+1,\alpha}(x_{n+1})$ at quantile level $\alpha \in (0, 1)$ of Y_{n+1} , given a new observation x_{n+1} is given by

$$\begin{aligned} Q_{n+1,\alpha}(x_{n+1}) &= \int F_Y^{-1}(\Phi_1(\varrho_{n+1,\alpha}(x_{n+1}))) p(\eta|y_{1:n}) d\eta, \text{ where} \\ \varrho_{n+1,\alpha}(x_{n+1}) &= \int [\Phi^{-1}(\alpha)/s - f_{\mathcal{E},\mathcal{M}}(x_{n+1})] p(\eta|y_{1:n}) d\eta, \end{aligned}$$

and we obtain estimates $\widehat{Q}_{n+1,\alpha}(x_{n+1})$ as we do for point and distributional predictions.

3 Estimation

3.1 Likelihood

The likelihood of the copula model is given by (8). To evaluate this requires inversion or factorization of the $(n \times n)$ matrix $\Omega(c, \mathcal{E}) = S_{1:n}(cEE^\top + I_n)S_{1:n}$. Direct evaluation involves $O(n^3)$ operations and is infeasible for typical sample sizes n .¹ To avoid this computation we instead employ an *extended likelihood* that augments with the leaf node values \mathcal{M} given by

$$\begin{aligned} p(y_{1:n}, \mathcal{M}|c, \mathcal{E}) &= p(y_{1:n}|\eta)\pi(\mathcal{M}|c, \mathcal{E}) \\ &= p(\tilde{z}_{1:n}|\eta) \prod_{i=1}^n \frac{p_Y(y_i)}{s\phi(z_i)} \prod_{j=1}^m \phi(M^j; 0, cI_{K^j}), \end{aligned}$$

where the second line follows from Proposition 1 with indices $A = \{1 : n\}$. Recall that the leaf node values were integrated out of the implicit copula model and are not copula parameters, and we stress their re-introduction to aid computation does not change this in any way. From (3), $p(\tilde{z}_{1:n}|\eta) = \prod_{i=1}^n \phi(\tilde{z}_i - f_{\mathcal{E}, \mathcal{M}}(x_i))$, and recall that $\tilde{z}_i = z_i/s = z_i\sqrt{1+mc}$, so that the extended likelihood is

$$p(y_{1:n}, \mathcal{M}|c, \mathcal{E}) \propto (1+mc)^{n/2} \prod_{i=1}^n \exp\left\{-\frac{(z_i \cdot \sqrt{1+mc} - f_{\mathcal{E}, \mathcal{M}}(x_i))^2 - z_i^2}{2}\right\} p_Y(y_i) \prod_{j=1}^m \phi(M^j; 0, cI_{K^j}),$$

which is fast to evaluate in $O(n)$ operations.

3.2 Posterior Evaluation

The posterior of the copula parameters $\{c, \mathcal{E}\}$ augmented with the leaf node values \mathcal{M} is

$$p(\eta|y_{1:n}) \propto p(y_{1:n}, \mathcal{M}|c, \mathcal{E})\pi(c, \mathcal{E}),$$

which is the product of the extended likelihood and prior. Conditional on the marginal F_Y , this can be evaluated efficiently using MCMC. A key observation is that the conditional posteriors $p(\mathcal{E}|c, \mathcal{M}, y_{1:n}) = p(\mathcal{E}|c, \mathcal{M}, \tilde{z}_{1:n})$ and $p(\mathcal{M}|c, \mathcal{E}, y_{1:n}) = p(\mathcal{M}|c, \mathcal{E}, \tilde{z}_{1:n})$, so they are the same as for the Gaussian BART model of the pseudo-response values specified in

¹The Woodbury identity can be used to factor Ω , but even so it still involves $O(nK^2 + K^3)$ computations where $K = \sum_{j=1}^m K^j$ where in our empirical work $m = 75$ and $1 \leq K^j \leq 5$ are typical, so the computation remains demanding.

Section 2.1. Therefore, the efficient and scalable steps outlined by Chipman et al. (2010), adjusted for the leaf node prior at (4), can be used to generate draws from these conditionals. Because these are the key computations in the MCMC scheme, this is why estimation of our copula process is almost as fast as for the original BART model.

What remains is the generation of the scalar c from its conditional posterior. To do so we transform c to the real line by taking the logarithm $\tilde{c} = \log(c)$ and use Hamiltonian Monte Carlo (HMC) with a leapfrog integrator and dual averaging (Nesterov; 2007). This requires evaluation of the logarithm of the conditional posterior and its gradient, for which closed form expressions can be derived as follows. The conditional posterior of c is

$$\begin{aligned} p(c \mid \mathcal{E}, \mathcal{M}, y_{1:n}) &\propto p(y_{1:n}, \mathcal{M} \mid c, \mathcal{E}) \pi(c) \\ &\propto (1 + mc)^{\frac{n}{2}} \cdot \exp \left\{ -\frac{\sum_{i=1}^n [(z_i \cdot \sqrt{1 + mc} - f_{\mathcal{E}, \mathcal{M}}(x_i))^2 - z_i^2]}{2} \right\} \\ &\quad \cdot \left[\prod_{h=1}^m \prod_{k=1}^{K_h} \frac{1}{\sqrt{c}} \exp \left(-\frac{\mu_{hk}^2}{2c} \right) \right] c^{-a-1} e^{-\frac{b}{c}}, \end{aligned}$$

from which it follows that the log-posterior $l_{\tilde{c}} = \log(p(\tilde{c} \mid \mathcal{E}, \mathcal{M}, y_{1:n}))$ is (up to an additive constant)

$$\begin{aligned} l_{\tilde{c}} &= \frac{n}{2} \log(1 + m \exp(\tilde{c})) - \frac{1}{2} (1 + m \exp(\tilde{c})) \sum_{i=1}^n z_i^2 + \sqrt{1 + m \exp(\tilde{c})} \sum_{i=1}^n z_i f_{\mathcal{E}, \mathcal{M}}(x_i) \\ &\quad - \frac{K\tilde{c}}{2} - \frac{\mu}{2 \exp(\tilde{c})} - a\tilde{c} - \tilde{c} - \frac{b}{\exp(\tilde{c})}, \end{aligned}$$

where $K = \sum_{h=1}^m K^h$ (K^h : Number of leaf nodes in tree h) and $\mu = \sum_{h=1}^m \sum_{k=1}^{K^h} (M_k^h)^2$ are the total number of leaf nodes and the sum of the square of all leaf node values, respectively.

The gradient of $l_{\tilde{c}}$ is

$$\begin{aligned} \frac{\partial l_{\tilde{c}}}{\partial \tilde{c}} &= \frac{nm \exp(\tilde{c})}{2(1 + m \exp(\tilde{c}))} - \frac{m \exp(\tilde{c})}{2} \sum_{i=1}^n z_i^2 + \frac{m \exp(\tilde{c})}{2\sqrt{1 + m \exp(\tilde{c})}} \sum_{i=1}^n z_i f_{\mathcal{E}, \mathcal{M}}(x_i) \\ &\quad - \frac{K}{2} + \frac{\mu}{2 \exp(\tilde{c})} - a - 1 + \frac{b}{\exp(\tilde{c})}. \end{aligned}$$

Algorithm 1 below gives the estimation algorithm for our CP-BART model.

Algorithm 1 CP-BART estimation algorithm

Require: Data $y_{1:n}$, burn-in size J_{burn} and Monte Carlo sample size J_{iter}

- 1: Fit KDE to the marginal distribution to obtain an estimate \hat{F}_Y for F_Y
 - 2: Compute the standardized pseudo-responses $z_i = \Phi^{-1}(\hat{F}_Y(y_i))$ for $i = 1, \dots, n$
 - 3: Initialize $\{\mathcal{E}^{[0]}, \mathcal{M}^{[0]}, c^{[0]}\}$ to feasible values
 - 4: Set $s^{[0]} = (1 + mc^{[0]})^{-1/2}$ and $\tilde{z}_i^{[0]} = z_i/s^{[0]}$ for $i = 1, \dots, n$
 - 5: **for** $j \leftarrow 1$ to $(J_{\text{iter}} + J_{\text{burn}})$ **do**
 - 6: Draw $\mathcal{E}^{[j]}$ from $p(\mathcal{E}|c^{[j-1]}, \mathcal{M}^{[j-1]}, \tilde{z}_{1:n}^{[j-1]})$ using the approach in Chipman et al. (2010)
 - 7: Draw $\mathcal{M}^{[j]}$ from $p(\mathcal{M}|c^{[j-1]}, \mathcal{E}^{[j]}, \tilde{z}_{1:n}^{[j-1]})$ using the approach in Chipman et al. (2010)
 - 8: Draw $c^{[j]}$ from $p(c|\mathcal{E}^{[j]}, \mathcal{M}^{[j]}, \tilde{z}_{1:n}^{[j-1]})$ using HMC
 - 9: Set $s^{[j]} = (1 + mc^{[j]})^{-1/2}$ and $\tilde{z}_i^{[j]} = z_i/s^{[j]}$ for $i = 1, \dots, n$
 - 10: **if** $j > J_{\text{burn}}$ **then**
 - 11: Collect $\{\mathcal{E}^{[j]}, \mathcal{M}^{[j]}, c^{[j]}\}$
 - 12: **end if**
 - 13: **end for**
 - 14: Output Monte Carlo Sample from $p(\eta|y_{1:n})$
-

4 Theoretical Results

In this section we establish posterior consistency for our CP-BART model. Under the same assumptions as in Ročková and van der Pas (2020) (see Appendix A for these) in Theorem 1 we prove posterior concentration for the regression function in the pseudo-response model (3) with the true regression function f_0 , where f_0 need not be a tree ensemble. While in our model f_0 is the regression function for the transformed variable \tilde{Z} , it also contributes to the dependence structure of our Gaussian copula process in (8). Thus, our posterior concentration result can be thought of as posterior concentration for modeling the effect of the covariates on the dependence structure of Y . Unlike previous results, we allow for a prior on the leaf node variances as in Section 2. In Theorem 2 we show convergence in distribution of the estimates for the predictive conditional distributions, and in Theorem 3 we show convergence of the conditional expectation, assuming that the tail decay of the response is sufficiently strong, as in Assumption B.

Theorem 1. *Assume that Assumptions (A1)–(A5) are fulfilled. Consider a BART model with a prior distribution $M_j^k \sim \mathcal{N}(0, c)$ on the leaf node coefficients where $c \sim \text{IG}(a, b)$, m and q fixed, $\sigma^2 = 1$ and the BART priors from Ročková and van der Pas (2020) on the other model parameters. The splitting probability at each node is given by $p_{\text{split}}(T^i) = \nu^{d(T^i)}$ for*

$\frac{1}{n} \leq \nu < \frac{1}{2}$. Denote by $\Pi(f)$ our BART prior on $f \in \mathcal{F}(\mathcal{E})$ as defined implicitly in Section 2.1. Then with $\varepsilon_n = n^{-\frac{\alpha}{2\alpha+q_0}} \log n$ we have

$$\Pi(f \in \mathcal{F}(\mathcal{E}) : \|f_0 - f\|_n > L_n \varepsilon_n \mid Y_{1:n}) \longrightarrow 0$$

for any $L_n \rightarrow \infty$ in probability, as $n, p \rightarrow \infty$.

The proof of Theorem 1 is provided in the Supplementary Material C.

Remark 2. Theorem 1 is similar to Theorem 7.1 of Ročková and van der Pas (2020), but also allows for inverse gamma priors on the variance of the Gaussian prior on the leaf nodes. Remarkably Ročková and Saha (2019) showed that the consistency result holds even if the number of parameters p is increasing. We stated the theorem here in this more general form, but note that it also holds in the special case of a fixed p which will be the setting we are working with.

Consider the estimated posterior predictive distribution $\hat{p}_{n+1}(y_{n+1}|\tilde{x})$ of a fixed covariate vector \tilde{x} defined in Section 2.3. Let $Y_{n+1}^{\tilde{x}}$ be a sample from this distribution, and let likewise $Y^{\tilde{x}}$ be a sample from the true conditional distribution $p(y|\tilde{x})$. The vector of transformed responses $Z_i = \Phi^{-1}(F_Y(Y_i))$ equals $s\tilde{Z}_i$ where $\tilde{Z}_i \sim N(f_0(X_i), 1)$ and $s = (1 + mc_0)^{-1}$ for some $c_0 \in (0, \infty)$. To establish the convergence of our distributional predictions, we need consistent estimators for f_0 and c_0 . We provide full proofs in the Supplementary Material D and E, and refer to Remark 3 below for the general proof strategy. Then, we have the following two convergence results.

Theorem 2. Assume that Theorem 1 holds and that \hat{F}_Y is a consistent estimator for the marginal distribution F_Y of Y , assume furthermore that we have consistent estimators for f_0 and c_0 . Then,

$$Y_{n+1}^{\tilde{x}} \xrightarrow{d} Y^{\tilde{x}} \quad \text{as } n \rightarrow \infty.$$

Furthermore, to show convergence of the point estimate of the conditional mean $\hat{Y}_{n+1}(\tilde{x})$ defined in Section 2.3 to the true conditional mean $\mathbb{E}(Y|\tilde{x})$, the following assumption is required.

Assumption B. Assume that the tails of Y satisfy:

$$\mathbb{P}(Y > t) \leq \Phi\left(-\frac{\log\left(\frac{t}{C}\right)}{B}\right), \quad \mathbb{P}(Y < -t) \leq \Phi\left(-\frac{\log\left(\frac{t}{C}\right)}{B}\right),$$

for some $B > 0, C > 0$ and for all $t \geq C$.

Theorem 3. *Assume that Theorem 1 holds, that Assumption B is fulfilled and that \hat{F}_Y is a consistent estimator for the marginal distribution F_Y of Y with inverse \hat{F}_Y^{-1} . Assume furthermore that we have consistent estimators for f_0 and c_0 . Then,*

$$\hat{Y}_{n+1}(\tilde{x}) \xrightarrow{p} \mathbb{E}(Y \mid \tilde{x}) \quad \text{as } n \rightarrow \infty.$$

The proofs of Theorems 2 and 3 are provided in the Supplementary Material F and G.

Remark 3. Theorems 2 and 3 require the existence of consistent point estimators. Such estimators are guaranteed when the posterior is itself consistent (see e.g. Proposition 6.7 in Ghosal and van der Vaart (2017)); however, for our model we are particularly interested in whether the posterior mean is consistent. Under additional assumptions on the behavior of f_0 , we establish posterior consistency for the model parameter c_0 and show that the posterior mean is indeed a consistent estimator. For estimation of f_0 we impose a condition on the growth of the posterior k -th moment for some $k > 1$ to ensure consistency of the posterior mean. Full details and proofs are provided in Supplementary Material D and E.

5 Simulation Study

We undertake a simulation study to demonstrate the efficacy of using CP-BART for distributional prediction.

5.1 Simulation Design

The data generating processes (DGPs) use the five-dimensional Friedman function (Friedman et al.; 1983)

$$f(x) := 10 \sin(\pi x_1 x_2) + 20 \left(x_3 - \frac{1}{2}\right)^2 + 10x_4 + 5x_5,$$

which exhibits nonlinearity and variable interactions. Let $x = (x_1, \dots, x_5)^\top$. The covariate values are first drawn $x_i \sim \mathcal{N}(0, \Sigma)$ independently for $i = 1, \dots, n$, with a Toeplitz

covariance structure $\Sigma_{lj} = \rho^{|l-j|}$, and then standardized to lie in the unit interval. Setting $\rho = 0.3$ produces a mildly correlated covariate vector. We further normalize the function by approximations of its mean and twice its standard deviation

$$f^*(x) := \frac{f(x) - 15}{2 \cdot \sqrt{5.5}}.$$

We sample from the following three distributions:

Case 1, Normal: $Y = f^*(x) + \varepsilon, \quad \varepsilon \sim \mathcal{N}(0, r_1^2).$

Case 2, Implicit Copula: $Y = F_{\text{Gamma}}^{-1}(\Phi(z); 3, 2), \quad z = f^*(x) + \varepsilon, \quad \varepsilon \sim \mathcal{N}(0, r_2^2)$

Case 3, Gamma: $Y = F_{\text{Gamma}}^{-1}\left(u; \frac{f(x)}{\sqrt{5.5}}, r_3\right), \quad u \sim U(0, 1).$

The scale values r_l^2 for $l = 1, 2, 3$ are chosen so that the signal-to-noise ratio (SNR) is approximately four in each case, making it simpler to compare results. The SNR is defined here as

$$\text{SNR} = \frac{\text{range}(\mathbb{E}(Y | x))}{(\int \text{Var}(Y | x) dx)^{\frac{1}{2}}},$$

from which the scales are computed to be $r_1^2 = 2.0787$, $r_2^2 = 1.6$ and $r_3^2 = 0.2601$; see the Supplementary Material H for details.

We simulate $R = 100$ replicates of training data from all three cases with sample sizes $n = 250, 500, 1000$. To measure the accuracy, for each case we generate one further test dataset $\{(y_i, x_i); i \in D\}$ with $|D| = n_{\text{test}} = 250$ observations. Results are based on $m = 75$ trees and 5000 MCMC iterations, including a burn-in phase of 1000 iterations giving us 4000 samples in total.

5.2 Evaluation Metrics

For each test dataset we compute the following three metrics. First, to assess the accuracy of point predictions $\hat{Y}_i(x_i)$ of the dependent variable, we compute the root mean square error,

$$\text{RMSE} = \sqrt{\frac{1}{n_{\text{test}}} \sum_{i \in D} (\hat{Y}_i(x_i) - y_i)^2}.$$

Second, to assess the accuracy of the predictive density $\widehat{p}_i(y_i|x_i)$ for the conditional distribution $Y_i|x_i$, we compute the mean log-score,

$$\text{LS} = -\frac{1}{n_{\text{test}}} \sum_{i \in D} \log \{\widehat{p}_i(y_i|x_i)\},$$

orientated so that lower values indicate greater accuracy. Third, because the true quantiles $Q_{i,\alpha}(x_i)$ can be computed from the DGP’s by simulation, we compute the RMSE between these and the predicted quantiles as a summary of their accuracy. That is, for a given quantile α we compute

$$\text{QRMSE}_\alpha = \sqrt{\frac{1}{n_{\text{test}}} \sum_{i \in D} \left(\widehat{Q}_{i,\alpha}(x_i) - Q_{i,\alpha}(x_i) \right)^2}.$$

Fourth, following Li et al. (2023), for estimation using MCMC we compute coverage of the 95% posterior predictive probability intervals for the quantiles $Q_{i,\alpha}(x_i)$ as follows. For a given observation $i \in D$ and value α , we use a sample from the parameter posterior to compute a sample $\{Q_{i,\alpha}(x_i)^{[1]}, \dots, Q_{i,\alpha}(x_i)^{[J_{\text{iter}}]}\}$ from the posterior of the quantiles. From the ordered sample, 95% probability intervals can be evaluated. Finally, we report the coverage of these intervals across the test data at $\alpha = 0.25, 0.5$ and 0.75 .

5.3 Benchmarks

The benchmarks for the proposed CP-BART model include the (i) original BART model with Gaussian errors of Chipman et al. (2010), (ii) SBART-DS model of Li et al. (2023), and (iii) “random forest conditional distribution estimation” (RFCDE) approach of Pospisil and Lee (2018). Mean, density and quantile predictions for CP-BART are obtained as described in Section 2.2. Predictions for BART are obtained in a similar manner using draws from the standard MCMC scheme. The SBART-DS model estimates conditional densities by tilting a base model (e.g., Gaussian) using a flexible function modeled with soft Bayesian additive regression trees. All three models are estimated using MCMC, from which coverage of the predicted quantiles can be computed.

RFCDE uses a random forest model designed for conditional density estimation. It modifies the traditional random forest algorithm by optimizing tree splits using a loss function tailored to conditional density estimation, from which mean and quantile predictions can

also be evaluated. However, this approach does not quantify the epistemic uncertainty of the estimates (e.g. by using either a posterior or sampling distribution) so that coverage of the predictions cannot be evaluated. For both SBART-DS and RFCDE we use the code provided by the authors.

Table 1: Predictive Accuracy Metrics for Simulation Case 1.

Method	QRMSE			Quantile Coverage			RMSE	LS
	$\alpha = 0.25$	$\alpha = 0.50$	$\alpha = 0.75$	$\alpha = 0.25$	$\alpha = 0.50$	$\alpha = 0.75$		
n = 250								
BART	0.64	0.64	0.64	0.96	0.96	0.96	0.64	2.18 ⁺⁺⁺
CP-BART	0.65	0.65	0.65	0.95	0.95	0.95	0.64	2.20
RFCDE	0.97 ^{***}	0.95 ^{***}	0.96 ^{***}	–	–	–	0.82 ^{***}	2.34 ^{***}
SBART-DS	0.71 ^{***}	0.71 ^{***}	0.72 ^{***}	0.83	0.82	0.81	0.71 ^{***}	2.18 ⁺⁺⁺
n = 500								
BART	0.57	0.57	0.57	0.96	0.96	0.96	0.57	2.17⁺⁺⁺
CP-BART	0.58	0.58	0.58	0.94	0.94	0.94	0.57	2.19
RFCDE	0.89 ^{***}	0.86 ^{***}	0.88 ^{***}	–	–	–	0.76 ^{***}	2.32 ^{***}
SBART-DS	0.66 ^{***}	0.67 ^{***}	0.67 ^{***}	0.75	0.74	0.73	0.67 ^{***}	2.17 ⁺⁺⁺
n = 1000								
BART	0.51	0.51	0.51	0.96	0.96	0.96	0.51	2.16 ⁺⁺⁺
CP-BART	0.51	0.51	0.51	0.94	0.95	0.94	0.51	2.17
RFCDE	0.82 ^{***}	0.80 ^{***}	0.82 ^{***}	–	–	–	0.70 ^{***}	2.30 ^{***}
SBART-DS	0.64 ^{***}	0.63 ^{***}	0.64 ^{***}	0.71	0.70	0.69	0.64 ^{***}	2.17 ⁺
n = 5000								
BART	0.43⁺⁺	0.43⁺⁺	0.43⁺⁺	0.95	0.95	0.95	0.43⁺⁺	2.15⁺⁺
CP-BART	0.44	0.44	0.44	0.92	0.92	0.91	0.44	2.15
RFCDE	0.73 ^{***}	0.71 ^{***}	0.73 ^{***}	–	–	–	0.63 ^{***}	2.27 ^{***}

Note: Methods and metrics are outlined in the text. Mean QRMSE, RMSE and LS values across all replicates are reported, with low values indicating higher accuracy and the lowest values in bold. Mean metrics significantly greater/smaller than CP-BART are marked with “***/+” (0.1% level), “**/+” (1% level) and “*/+” (5% level). Quantile coverage is at the 95% level for three quantile values $\alpha = 0.25, 0.5$ and 0.75 . Coverage is not reported for RFCDE as the method does not quantify epistemic uncertainty, while SBART-DS is not reported for the sample size $n = 5000$ due to high computational demand.

5.4 Results

Tables 1, 2, and 3 present the evaluation metrics for the three cases, with results given for different sample sizes and methods. The ranking of the methods by speed (from fastest to slowest) is RFCDE, BART, CP-BART and SBART-DS. For example, predictions were

obtained for a dataset of size $n = 5000$ for the methods in this order in an average of 14.5s, 41.8s, 47.5s and 2092s; see Table I.4 in the Supplementary Material for a comparison of speed with increasing n/p . The fast speed of CP-BART is because Algorithm 1 involves only inexpensive additional computations over-and-above that for BART, which is well-known for its scalability. Because of its higher computational time, results are not reported for SBART-DS when $n = 5000$.

Table 2: Predictive Accuracy Metrics for Simulation Case 2.

Method	RMSE $_Q$			Quantile Coverage			RMSE	LS
	$\alpha = 0.25$	$\alpha = 0.50$	$\alpha = 0.75$	$\alpha = 0.25$	$\alpha = 0.50$	$\alpha = 0.75$		
n = 250								
BART	0.36***	0.56***	0.67***	0.99	0.90	0.81	0.37***	1.94***
CP-BART	0.20	0.32	0.47	0.94	0.94	0.94	0.34	1.56
RFCDE	0.33***	0.52***	0.76***	–	–	–	0.49***	1.76***
SBART-DS	0.25***	0.42***	0.58***	0.76	0.71	0.81	0.40***	1.61***
n = 500								
BART	0.36***	0.54***	0.61***	0.96	0.85	0.78	0.34***	1.94***
CP-BART	0.18	0.29	0.42	0.93	0.93	0.93	0.31	1.55
RFCDE	0.31***	0.48***	0.74***	–	–	–	0.47***	1.73***
SBART-DS	0.23***	0.37***	0.50***	0.69	0.71	0.84	0.35***	1.59***
n = 1000								
BART	0.37***	0.52***	0.59***	0.94	0.79	0.72	0.30***	1.93***
CP-BART	0.15	0.24	0.36	0.94	0.94	0.95	0.26	1.54
RFCDE	0.29***	0.46***	0.70***	–	–	–	0.45***	1.70***
SBART-DS	0.20***	0.33***	0.46***	0.69	0.74	0.85	0.33***	1.56***
n = 5000								
BART	0.34***	0.49***	0.54***	0.86	0.55	0.52	0.26***	1.93***
CP-BART	0.13	0.20	0.30	0.92	0.92	0.92	0.22	1.53
RFCDE	0.24***	0.42***	0.68***	–	–	–	0.44***	1.68***

See note to Table 1 for table description.

In Case 1 the DGP has an additive Gaussian error, matching the BART model, so that this method is most accurate in Table 1. However, of the three distributional regression methods, CP-BART is most accurate by all measures, except for LS where SBART-DS is superior. In Case 2 the data are generated from a transformation of a latent nonlinear regression with Gaussian disturbances. This is a Gaussian copula process model, so that CP-BART should perform well here. It does so in Table 2, dominating the other approaches on all metrics and at all sample sizes. In Case 3 the DGP has a highly non-Gaussian

Table 3: Predictive Accuracy Metrics for Simulation Case 3.

Method	RMSE _Q			Quantile Coverage			RMSE	LS
	$\alpha = 0.25$	$\alpha = 0.50$	$\alpha = 0.75$	$\alpha = 0.25$	$\alpha = 0.50$	$\alpha = 0.75$		
n = 250								
BART	1.03***	1.11***	1.23***	0.98	0.98	0.96	0.97***	2.65***
CP-BART	0.51	0.73	1.03	0.96	0.94	0.91	0.79	2.44
RFCDE	0.89***	1.11***	1.49***	–	–	–	1.00***	2.60***
SBART-DS	0.64***	0.87***	1.15***	0.94	0.90	0.86	0.88***	2.48***
n = 500								
BART	0.98***	1.02***	1.11***	0.97	0.97	0.96	0.87***	2.64***
CP-BART	0.44	0.62	0.89	0.96	0.95	0.92	0.68	2.43
RFCDE	0.84***	1.05***	1.39***	–	–	–	0.93***	2.59***
SBART-DS	0.60***	0.81***	1.05***	0.91	0.88	0.86	0.81***	2.47***
n = 1000								
BART	0.92***	0.97***	1.06***	0.96	0.95	0.94	0.79***	2.64***
CP-BART	0.40	0.57	0.82	0.95	0.93	0.90	0.62	2.43
RFCDE	0.77***	0.98***	1.30***	–	–	–	0.87***	2.57***
SBART-DS	0.56***	0.76***	1.01***	0.88	0.86	0.85	0.77***	2.46***
n = 5000								
BART	0.77***	0.82***	0.92***	0.90	0.85	0.80	0.61***	2.62***
CP-BART	0.33	0.46	0.68	0.94	0.92	0.86	0.51	2.43
RFCDE	0.70***	0.88***	1.15***	–	–	–	0.79***	2.57***

See note to Table 1 for table description.

response distribution that varies with covariate values, but is not a copula process model. As expected, in Table 3 the three distributional regression methods clearly out-perform the BART model which only allows the conditional mean to vary with covariates. Of these, CP-BART dominates throughout, followed by SBART-DS and then RFCDE.

We make two additional observations on CP-BART. First, it estimates the conditional quantiles very well, both in terms of point forecast accuracy measured by QRMSE and with well-calibrated coverage. This is despite the method not being a tailored quantile regression approach. Second, similar to the original BART model, we tried fixing the scale of the leaf nodes c to a constant ($\frac{9}{7m}$, see Section 2.2 for details), but this reduced the predictive accuracy. This is because c is crucial when estimating the copula process parameter matrix $\Omega(c, \mathcal{E})$, and its posterior can differ meaningfully for any given dataset. The corresponding evaluation metrics can be found in Tables I.1–I.3 of the Supplementary Material.

6 Real World Data Illustrations

We evaluate our CP-BART and the benchmark methods considered in Section 5 on the five real world regression datasets listed in Table 6. All datasets but the Rain data (which is from the R-package `disttree`) were obtained from the UCI repository. The datasets vary in sample size and number of covariates, so that they represent a variety of circumstances. All are where the relationship between the covariates and the response is possibly nonlinear and not additive, with a response distribution that is non-Gaussian and may be covariate dependent. Thus, distributional regression tree models are an attractive choice. Further implementation details are given in Supplementary Material J.

Table 4: Five Real World Regression Datasets

Dataset	Source	n	p	Response Variable (y)
Housing	UCI-NoID	506	12	Median value of owner-occupied homes (USD 1,000)
Rain	R-disttree	867	82	Power transformed observed total precipitation ($\text{mm}^{\frac{1}{1.6}}$)
Concrete	UCI-ID165	1,030	8	Concrete compressive strength (MPa)
Bike	UCI-ID275	17,379	12	Bike rentals (count)
Music	UCI-ID203	515,345	90	Release year of songs

6.1 CP-BART Results

Each dataset was fit using CP-BART and we make three observations. First, c is a key parameter in the copula process, and plots of MCMC draws of it are an effective diagnostic of convergence of the sampler. These are given in Figure J.1 in the Supplementary Material, and visual inspection suggests convergence is fast for the three smaller datasets, although more draws are necessary for the large Bike and Music datasets. Second, Figure 1 plots the predictive densities for three representative observations in the Rain and Bike datasets. This includes the posterior mean of the predictive densities, and there is strong variability in the shape of the predictive densities across observations. Thus, accounting for the covariate values through the copula process, and not through the marginal p_Y , at (8) is impactful. Third, also plotted are 90% posterior probability intervals for the densities. This is obtained by

evaluating the predictive densities at draws from $p(\eta|y)$, instead of integrating out posterior uncertainty as in (10). The densities for the Rain dataset exhibit high epistemic uncertainty, which reflects its low sample size to variable ratio. In contrast, the posterior intervals are narrow for the Bike dataset, reflecting the high sample size to variable ratio for this case.

Predicted conditional densities with 5%–95% Confidence Bands

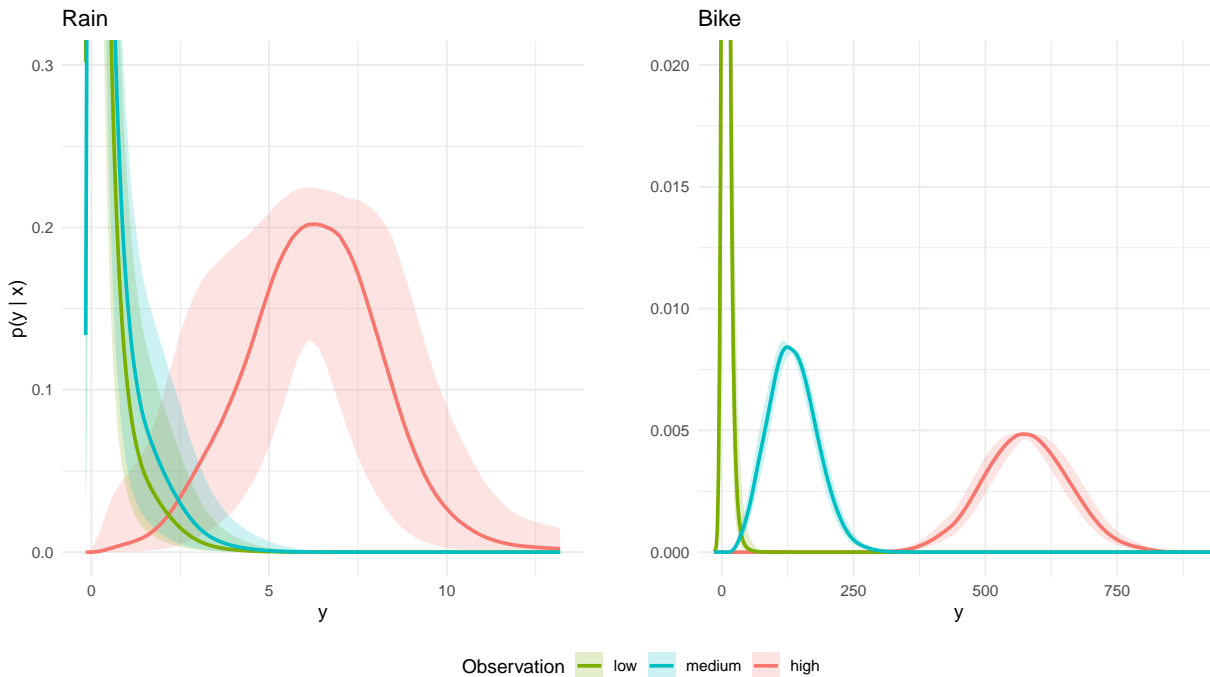


Figure 1: Predictive densities from CP-BART for the Rain (lefthand panel) and Bike (right-hand panel) datasets. For each dataset, predictions are made for the three observations corresponding the 5th, 50th and 95th percentiles of the response variable. Solid lines depict the posterior median of the predictive densities, while the shaded areas give the 90% posterior predictive probability intervals.

6.2 Comparison of Predictive Accuracy

To compare the predictive accuracy of the four models we compute the predictive (i) pinball loss (also called the quantile score), (ii) continuous ranked probability score (CRPS; Gneiting and Raftery; 2007) and (iii) log-scores, using 10-fold cross-validation as follows. For a given dataset, the data are randomly partitioned into ten (approximately) equal sized disjoint sub-samples. Each sub-sample has observation indices $B^{(k)}$ for $k = 1, \dots, 10$, so that $\bigcup_{k=1}^{10} B^{(k)} = \{1, 2, \dots, n\}$. For each sub-sample k , a model is fit using the other nine sub-samples as

training data, and the predictive densities $\hat{p}_i(y_i|x_i)$ and quantile functions $\widehat{Q}_{i,\alpha}(x_i)$ evaluated for $i \in B^{(k)}$ which are treated as test data. This is repeated for each partition $k = 1, \dots, 10$ and the metrics evaluated across all observations.

The pinball loss is defined at quantile α as $\text{PL}(\alpha) = \frac{1}{n} \sum_{i=1}^n \text{PL}_{i,\alpha}(y_i|x_i)$, where

$$\text{PL}_{i,\alpha}(y_i|x_i) := \left(\mathbb{1} \left(y_i < \widehat{Q}_{i,\alpha}(x_i) \right) - \alpha \right) \cdot \left(\widehat{Q}_{i,\alpha}(x_i) - y_i \right),$$

and the indicator function $\mathbb{1}(X) = 1$ if X is true, and zero otherwise. The CRPS is the integral of the pinball loss over all quantiles

$$\text{CRPS}(y_i) = 2 \int_0^1 \text{PL}_{i,\alpha}(y_i|x_i) d\alpha,$$

and we compute the mean over all observations. Cross-validation is used for four of the datasets, but not for the largest Music dataset because it has a pre-specified train/test split (463,715/51,630) that avoids the “producer effect” meaning no songs are from the same artist in both the test and training data.

Table 5: Predictive Accuracy for the Real World Datasets

Method	Housing	Rain	Concrete	Bike	Music
CRPS					
BART	1.60	0.85***	2.31	18.76***	4.88***
CP-BART	1.51	0.67	2.20	17.09	4.41
RFCDE	1.81*	0.69	3.08***	19.70***	4.65***
SBART-DS	2.00***	NI	4.47***	CD	CD
Log-score					
BART	2.76	1.83***	2.98	5.16***	3.63***
CP-BART	2.50	0.81	2.91	4.65	3.24
RFCDE	2.49	1.38***	3.07*	NI	3.10 +++
SBART-DS	2.67	NI	3.48***	CD	CD

Note: Mean metric values are reported, computed using 10-fold CV as described in the text. Lower values correspond to higher accuracy, with the lowest in bold. Mean metrics significantly greater/smaller than CP-BART are marked with “***/+” (0.1% level), “**/+” (1% level) and “*/+” (5% level). The acronym “CD” indicates computationally difficult to evaluate on standard machines, while “NI” indicates numerical instabilities were encountered when employing the code.

Table 5 reports the predictive CRPS and LS values. Results are not given for SBART-DS for the two largest datasets (Bike and Music) due to computational hurdles, and for the Rain dataset where the the code encountered numerical instabilities due to the challenging

n -to- p ratio. CP-BART is most accurate throughout when measured by CRPS, and for three datasets by LS. Only for two datasets (Housing and Music) RFCDE is more accurate than CP-BART, and with Housing the scores are not significantly different.

Figure 6.2 plots the pinball loss functions $PL(\alpha)$. These show that the CP-BART provides more accurate predictions than the three benchmark methods at all quantiles for all five datasets. To illustrate why this is case, Figure 3 plots the predictive densities for each method and four observations in the Housing data. The observations correspond to one of the cheapest, one of the most expensive and a median priced property tract, along with that with the lowest crime rate. Care was taken to fit the models to the data excluding these observations, so that the predictions are out-of-sample. All four densities from CP-BART are smoother, better located, and/or sharper than the benchmarks. Their shape also varies greatly over observation, showing how the copula process is responsive to covariate values.

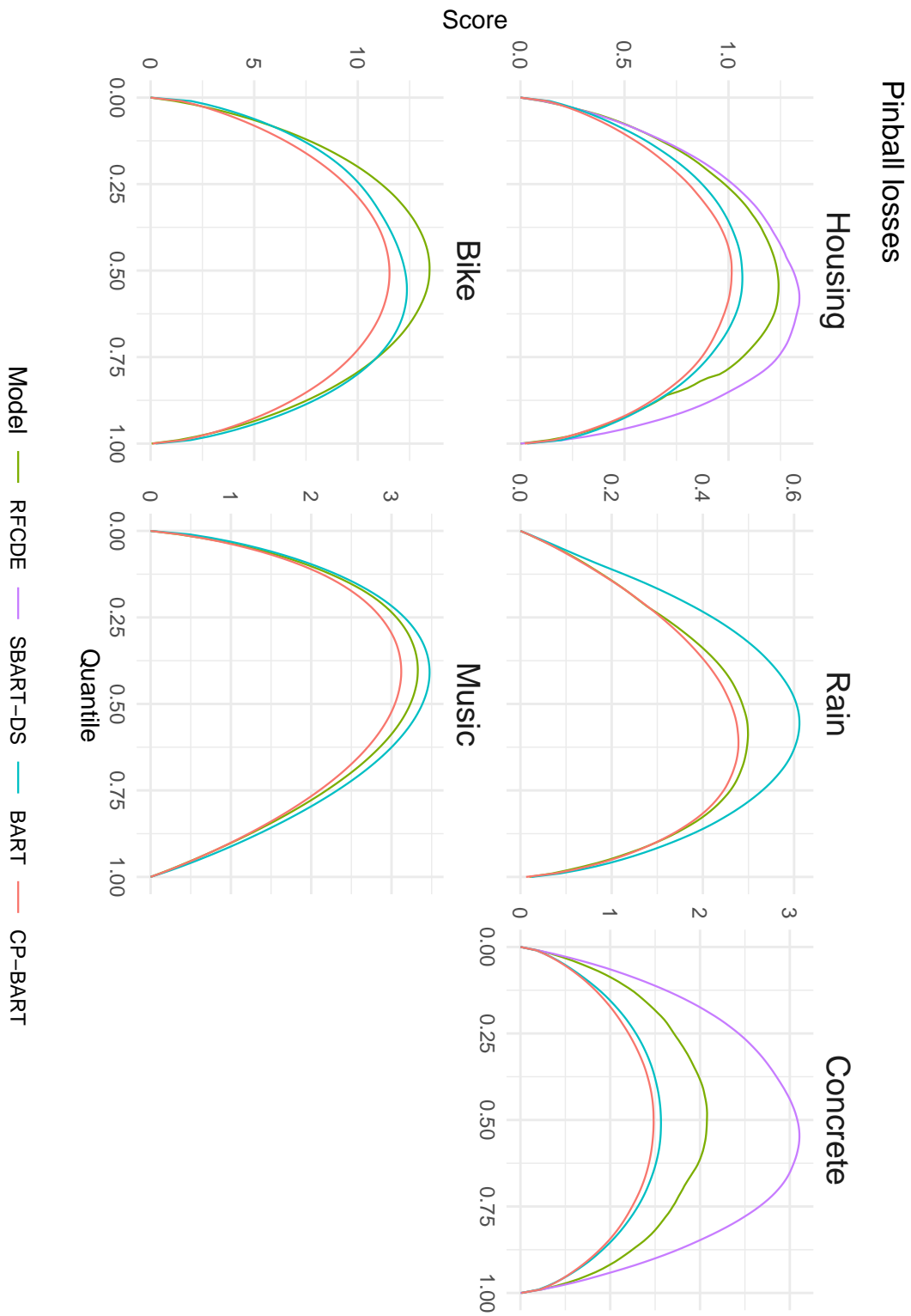


Figure 2: Pinball loss functions $PL(\alpha)$ plotted against quantile α for the five real-world datasets. The loss functions for the first four datasets are computed using 10-fold cross validation, and for the single pre-specified split for Music, as outlined in the text. Lower values correspond to increased accuracy.

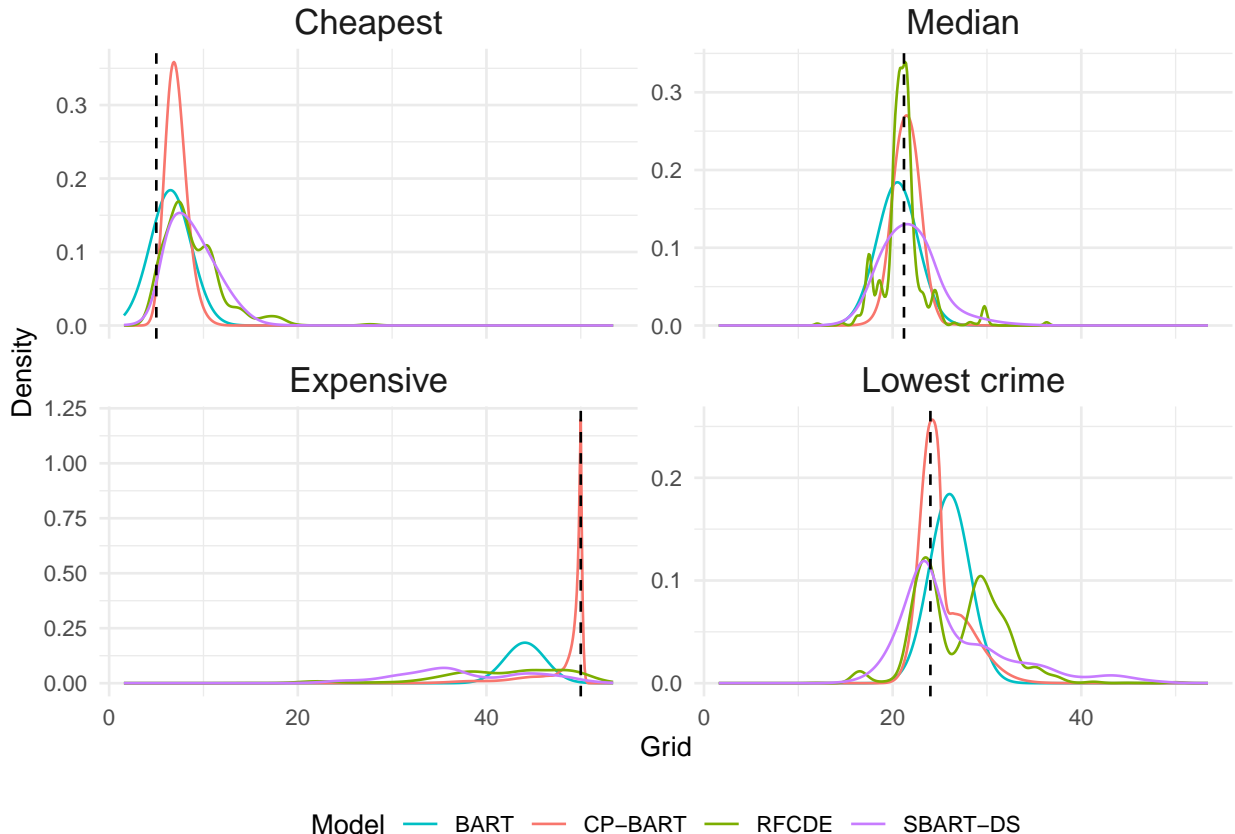


Figure 3: The plot shows the out-of-sample predicted conditional distributions across all methods for four different observations in the Housing dataset. The models were trained on all remaining data. The dashed vertical lines mark the observations.

7 Discussion

This paper is the first to show how to construct a Gaussian copula process from a BART model, and how it provides a robust and effective approach to extend BART to distributional regression. To do so, we make the following four contributions.

First, Proposition 1 shows that the copula process model is connected to the BART model for the pseudo-responses by an optimal transport map. This map is used to derive computationally efficient expressions for the conditional predictive distribution at (10), as well as the conditional mean and quantile functions. Second, our theoretical results extend those of Ročková and Saha (2019) by establishing posterior consistency of the regression function in a BART model that incorporates a prior on the leaf node variances. The latter

is necessary to define the flexible copula process. Furthermore, under additional regularity conditions, we prove convergence in distribution of the predictive conditional distribution and the conditional expectation, assuming the existence of consistent estimators for f_0 and c_0 . These estimators exist under posterior consistency, and we show that, given a growth condition on the posterior moments of f , the posterior means can be used for estimation.

Third, while evaluating the posterior directly is computationally demanding, it can be made tractable by augmenting the likelihood with the leaf node values \mathcal{M} . Although we stress that the implicit copula is strictly formed with \mathcal{M} integrated out; its reintroduction here is purely because the resulting augmented posterior can be evaluated using an MCMC sampler that exploits the fast sampling steps in Chipman et al. (2010). Thus, like the original BART algorithm, CP-BART is scalable with respect to sample size n , number of trees m and number of covariates p . Fourth, the simulation studies and five real data examples demonstrate scalability, accuracy of the predictive density, and both the accuracy and well-calibrated coverage of the conditional quantile function. In these empirical examples, CP-BART dominates the original Gaussian BART model, the distributional random forest method of Pospisil and Lee (2018) and the distributional regression BART model of Li et al. (2023). It provides sharp posterior probability intervals that maintain the desired coverage throughout.

Extending modern machine learning methods to distributional regression is a topic of substantial interest; for examples, see Schlosser et al. (2019) and Duan et al. (2020). The CP-BART model contributes to this literature. It extends and refines the work by Klein and Smith (2019) and Smith and Klein (2021) for a regularized linear regression model to the nonparametric BART model. It also the first paper to lay the theoretical foundations of such implicit Gaussian copula processes. The CP-BART model is also related to the approach of Kowal and Wu (2025), who propose to efficiently estimate the joint posterior of parametric regressions and unknown transformations using the Bayesian bootstrap. In contrast, the focus here is on forming the copula process model using an optimal transport map, and computing inference using an efficient MCMC sampler for an augmented posterior. Like the recently proposed alternative methods of Li et al. (2023) and O’Hagan and Ročková (2025), CP-BART demonstrates the potential of BART not only for point prediction, but

also for distributional prediction.

We finish by highlighting directions for future work. By considering different specifications for the BART model at (1), different copula processes can be derived. For example, Um et al. (2023) consider extending BART to allow for skew normal disturbances and an N -dimensional multivariate response variable. The former leads to a skew normal copula process, which can capture asymmetric dependence between response values. Such a copula process can be estimated using an extension of our MCMC scheme by exploiting the conditionally Gaussian representation of the skew normal distribution as in Deng et al. (2025). The latter extends the copula at (6) to Nn dimensions that captures both cross-variable and inter-observation dependence. However, this requires specification of a suitable prior on the leaf nodes, which are integrated out to construct the copula process. Finally, more complex BART model specifications also have implicit copula processes, but with more parameters and posteriors that may be more difficult to traverse using MCMC. In this case, exploring the application of variational inference techniques to compute approximate posterior inference at scale may be attractive.

References

- Basak, P., Linero, A., Sinha, D. and Lipsitz, S. (2022). Semiparametric analysis of clustered interval-censored survival data using soft Bayesian additive regression trees (SBART), *Biometrics* **78**(3): 880–893.
- Bissiri, P. G., Holmes, C. C. and Walker, S. G. (2016). A general framework for updating belief distributions, *Journal of the Royal Statistical Society Series B: Statistical Methodology* **78**(5): 1103–1130.
- Chipman, H. A., George, E. I. and McCulloch, R. E. (2010). BART: Bayesian additive regression trees, *The Annals of Applied Statistics* **4**(1): 266–298.
- Chipman, H. A., George, E. I., McCulloch, R. E. and Shively, T. S. (2022). mBART: Multidimensional monotone BART, *Bayesian Analysis* **17**(2): 515–544.

- Deng, L., Smith, M. S. and Maneesoonthorn, W. (2025). Large skew-t copula models and asymmetric dependence in intraday equity returns, *Journal of Business & Economic Statistics* **43**(2): 269–285.
- Duan, T., Avati, A., Ding, D. Y., Thai, K. K., Basu, S., Ng, A. Y. and Schuler, A. (2020). Ngboost: Natural gradient boosting for probabilistic prediction, in H. D. III and A. Singh (eds), *Proceedings of the 37th International Conference on Machine Learning*, Vol. 119 of *Proceedings of Machine Learning Research*, PMLR, pp. 2690–2700.
- Friedman, J. H., Grosse, E. and Stuetzle, W. (1983). Multidimensional additive spline approximation, *SIAM Journal on Scientific and Statistical Computing* **4**(2): 291–301.
- Ghosal, S. and van der Vaart, A. (2017). *Fundamentals of Nonparametric Bayesian Inference*, Cambridge University Press.
- Ghosh, D., Sinha, D., Linero, A. R. and Rust, G. (2024). Analysis of spatially clustered survival data with unobserved covariates using SBART, *arXiv:2411.06591* .
- Gneiting, T. and Raftery, A. E. (2007). Strictly proper scoring rules, prediction, and estimation, *Journal of the American Statistical Association* **102**(477): 359–378.
- Hahn, P. R., Murray, J. S. and Carvalho, C. M. (2020). Bayesian regression tree models for causal inference: Regularization, confounding, and heterogeneous effects (with discussion), *Bayesian Analysis* **15**(3): 965–1056.
- He, J., Hahn, P. R. and Yalov, H. F. L. (2019). XBART: Accelerated Bayesian additive regression trees, *The 22nd International Conference on Artificial Intelligence and Statistics (AISTATS)*, Vol. 89 of *Proceedings of Machine Learning Research*, PMLR, pp. 1130–1139.
- Hill, J. L., Scott, M. and Ricciardi, E. A. (2013). Bayesian nonparametric modeling for causal inference, *Journal of Computational and Graphical Statistics* **22**(4): 900–917.
- Hill, J., Linero, A. and Murray, J. (2020). Bayesian additive regression trees: A review and look forward, *Annual Review of Statistics and Its Application* **7**(1): 251–278.

- Kapelner, J. and Bleich, J. (2016). Prediction with Bayesian additive regression trees in the R package `bartMachine`, *Journal of Statistical Software* **70**(4): 1–40.
- Klein, N. (2024). Distributional regression for data analysis, *Annual Review of Statistics and Its Application* **11**: 321–346.
- Klein, N. and Kneib, T. (2016). Scale-dependent priors for variance parameters in structured additive distributional regression, *Bayesian Analysis* **11**(4): 1071–1106.
- Klein, N. and Smith, M. S. (2019). Implicit copulas from bayesian regularized regression smoothers, *Bayesian Analysis* **14**(4): 1143–1171.
- Kolesárová, A., Mesiar, R. and Sempi, C. (2008). Measure-preserving transformations, copulae and compatibility, *Mediterranean Journal of Mathematics* **5**(3): 325–339.
- Kowal, D. R. and Wu, B. (2025). Monte carlo inference for semiparametric bayesian regression, *Journal of the American Statistical Association* **120**(550): 1063–1076.
- Li, Y., Linero, A. R. and Murray, J. S. (2023). Adaptive conditional distribution estimation with Bayesian decision tree ensembles, *Journal of the American Statistical Association* **118**(543): 2129–2142.
- Linero, A. R. (2018). Bayesian regression trees for high-dimensional prediction and variable selection, *Journal of the American Statistical Association* **113**(522): 626–636.
- Linero, A. R. (2025). Generalized Bayesian additive regression trees models: Beyond conditional conjugacy, *Journal of the American Statistical Association* **120**(549): 356–369.
- Linero, A. R., Basak, P., Li, Y. and Sinha, D. (2022). Bayesian survival tree ensembles with submodel shrinkage, *Bayesian Analysis* **17**(3): 997–1020.
- Linero, A. R. and Daniels, M. J. (2015). A flexible Bayesian approach to monotone missing data in longitudinal studies with nonignorable missingness with application to an acute schizophrenia clinical trial, *Journal of the American Statistical Association* **110**(509): 45–55.

- Linero, A. R. and Du, J. (2023). Gibbs priors for Bayesian nonparametric variable selection with weak learners, *Journal of Computational and Graphical Statistics* **32**(3): 1046–1059.
- Linero, A. R. and Yang, Y. (2018). Bayesian regression tree ensembles that adapt to smoothness and sparsity, *Journal of the Royal Statistical Society: Series B (Statistical Methodology)* **80**(5): 1087–1110.
- Nesterov, Y. (2007). Primal-dual subgradient methods for convex problems, *Mathematical Programming* **120**(1): 221–259.
- O’Hagan, S. and Ročková, V. (2025). Generative regression with IQ-BART, *arXiv:2507.04168* .
- Orlandi, V., Murray, J., Linero, A. and Volfovsky, A. (2021). Density regression with Bayesian additive regression trees, *arXiv:2112.12259* .
- Pospisil, T. and Lee, A. B. (2018). RFCDE: Random forests for conditional density estimation, *arXiv:1804.05753* .
- Pratola, M. T., George, E. I. and McCulloch, R. E. (2024). Influential observations in Bayesian regression tree models, *Journal of Computational and Graphical Statistics* **33**(1): 47–63.
- Ročková, V. and Saha, E. (2019). On theory for BART, in K. Chaudhuri and M. Sugiyama (eds), *Proceedings of the Twenty-Second International Conference on Artificial Intelligence and Statistics*, Vol. 89 of *Proceedings of Machine Learning Research*, PMLR, pp. 2839–2848.
- Ročková, V. and van der Pas, S. (2020). Posterior concentration for Bayesian regression trees and forests, *The Annals of Statistics* **48**(4): 2108–2131.
- Scarpone, M., Kapelner, J. and Bleich, J. (2020). Bayesian additive regression trees for spatial modeling of COVID-19 incidence, *Spatial Statistics* **40**: 100434.
- Schapire, R. E. (1990). The strength of weak learnability, *Machine Learning* **5**(2): 197–227.

- Schlosser, L., Hothorn, T., Stauffer, R. and Zeileis, A. (2019). Distributional regression forests for probabilistic precipitation forecasting in complex terrain, *Annals of Applied Statistics* **13**(3): 1564–1589.
- Smith, M. S. (2023). Implicit copulas: An overview, *Econometrics and Statistics* **28**: 81–104.
- Smith, M. S. and Klein, N. (2021). Bayesian inference for regression copulas, *Journal of Business & Economic Statistics* **39**(3): 712–728.
- Song, P. X.-K. (2000). Multivariate dispersion models generated from Gaussian copula, *Scandinavian Journal of Statistics* **27**(2): 305–320.
- Um, S., Linero, A. R., Sinha, D. and Bandyopadhyay, D. (2023). Bayesian additive regression trees for multivariate skewed responses, *Statistics in Medicine* **42**(3): 246–263.
- Wang, Y., Linero, A. R. and MacEachern, S. N. (2022). Gibbs priors for Bayesian non-parametric variable selection with weak learners, *Journal of Computational and Graphical Statistics* **31**(4): 1241–1253.

A Assumptions for Theorems 1–3

The following Assumptions are required for the proof of Theorem 1 and are identical to those for Theorem 7.1 in Ročková and Saha (2019).

Assumption A. *Assume that:*

(A1) *The function f_0 is α -Hölder continuous with $0 < \alpha \leq 1$.*

(A2) *The function f_0 depends on a subset of the covariates $\mathcal{Q}_0 \subseteq \mathcal{Q}$ with $0 < q_0 := |\mathcal{Q}_0|$.*

(A3) *The function f_0 fulfills $\|f_0\|_\infty \lesssim \log^{\frac{1}{2}} n$.*

(A4) *The data \mathcal{X} is (W, \mathcal{Q}_0) regular (see Definition B.1 in the Supplementary Material).*

(A5) *The number of covariates p fulfills $\log p \lesssim n^{\frac{q_0}{2\alpha+q_0}}$.*